Reliability Testing the Die-Attach of CPV Cell Assemblies

Nick Bosco, Cassi Sweet, and Sarah Kurtz

Presented at the 34th IEEE Photovoltaic Specialists Conference (PVSC '09)
Philadelphia, Pennsylvania
June 7-12, 2009

Conference Paper
NREL/CP-5200-46058
February 2011

Contract No. DE-AC36-08GO28308

NOTICE

Available electronically at http://www.osti.gov/bridge

Available for a processing fee to U.S. Department of Energy
and its contractors, in paper, from:

U.S. Department of Energy
Office of Scientific and Technical Information

P.O. Box 62
Oak Ridge, TN 37831-0062
phone: 865.576.8401
fax: 865.576.5728
email: mailto:reports@adonis.osti.gov

Available for sale to the public, in paper, from:

U.S. Department of Commerce
National Technical Information Service
5285 Port Royal Road
Springfield, VA 22161
phone: 800.553.6847
fax: 703.605.6900
email: orders@ntis.fedworld.gov
online ordering: http://www.ntis.gov/help/ordermethods.aspx

Cover Photos: (left to right) PIX 16416, PIX 17423, PIX 16560, PIX 17613, PIX 17436, PIX 17721

Printed on paper containing at least 50% wastepaper, including 10% post consumer waste.

Reliability Testing the Die-Attach of CPV Cell Assemblies

Nick Bosco, Cassi Sweet and Sarah Kurtz

National Renewable Energy Laboratory, Golden, CO 80401

ABSTRACT

Results and progress are reported for a course of work to establish an efficient reliability test for the die-attach of CPV cell assemblies. Test vehicle design consists of a ~1 cm^2 multijunction cell attached to a substrate via several processes. A thermal cycling sequence is developed in a test-to-failure protocol. Methods of detecting a failed or failing joint are prerequisite for this work; therefore both in-situ and non-destructive methods, including infrared imaging techniques, are being explored as a method to quickly detect non-ideal or failing bonds.

INTRODUCTION

Concentrator photovoltaic (CPV) cell assemblies have been observed to fail at the points of attachment between the cell and heat-sink. If even small voids exist or form in die-attach material that composes these joints, catastrophic failure may occur. While the current IEC 62108 qualification test includes a temperature cycling sequence with the intention of accelerating these failures, the test is slow and may not detect a failed or failing joint because the pass criterion characterizes the cell rather than the joint. Furthermore, results cannot be extrapolated into device lifetime. There also remains controversy on the application of forward bias during this test. While large forward bias currents simulate how heat enters the assembly well, the current is not distributed similarly as while on-sun and may cause unintended and unrepresentative failure of the cell.

The current paper aims to detail the knowledge required to develop a CPV die-attach reliability test. First, the theory on how best to design and interpret a thermal cycling sequence for concentrator cell assemblies is discussed. This will include guidelines on how temperature parameters, ramp rates and dwell times influence the test's acceleration factor and overall test time. Second, the philosophy followed to develop a meaningful and efficient qualification test is presented. Finally, a novel technique for the thermal cycling of concentrator cell assemblies is presented, including chamber design, functionality and system monitoring. This section also includes an infrared method for detecting die-attach voids and packaging failures.

THERMAL CYCLING THEROY

There are two objectives with any thermal cycling sequence: (i) maximize the acceleration factor and (ii) draw conclusions about product reliability at use conditions. To realize these objectives it is necessary to establish a relationship between the parameters of the product life distribution and the applied stress.

A thermal cycling sequence consists of four key parameters, each of which will influence the acceleration factor, and are addressed here. They are ΔT (temperature amplitude), dwell time, cycle frequency and ramp rate. Low-cycle fatigue is the prominent mechanism for die-attach failures and is the accumulation of inelastic strain energy in the joint. The accumulation of inelastic strain energy in a die-attach layer for one thermal cycle is depicted schematically in a plot of shear stress vs. displacement, Fig. 1. The curve originates at the origin and moves towards point "A" at the maximum cycle temperature. During the high temperature dwell, further displacement may be achieved as the stress is relaxed through creep. Upon cooling the magnitude of stress increases and reaches its maximum at the cold dwell temperature, point "B". After subsequent heating to complete the cycle a hysteresis is achieved, the area of which is the inelastic strain energy accumulated for that cycle. Also included in the figure is the case if the die-attach remains elastic. Accordingly, there is no energy accumulation in the elastic limit.

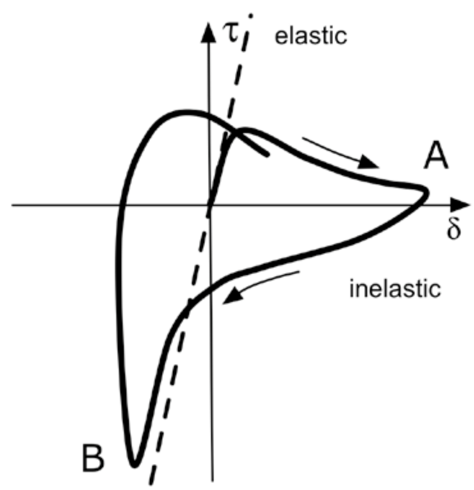

Fig. 1. Schematic elastic and inelastic stress-displacement response of a die-attach through thermal cycling.

Fatigue life is classically modeled by a power law between the number of stress cycles to failure, N_f, and the amplitude of that stress, $\Delta\sigma$ [1]:

$$N_f = C(\Delta\sigma)^{-n} \qquad (1)$$

where C is a constant. Recognizing that through thermal cycling the significant metric is inelastic strain amplitude,

$\Delta\varepsilon_p$, which is related to the temperature amplitude of test, ΔT, by the coefficient of thermal expansion (CTE) mismatch, $\Delta\alpha$. Equation (1) becomes:

$$N_f = C(\Delta T)^{-n} \tag{2}$$

assuming the CTE mismatch is constant. This expression is known as the Coffin-Manson equation [2]. When applied to an accelerated thermal cycling sequence, it may be re-written to define the acceleration factor of the test:

$$AF = \frac{N_{use}}{N_{test}} = \left(\frac{\Delta T_{use}}{\Delta T_{test}}\right)^{-n} \tag{3}$$

Accurate knowledge of the power law coefficient, n, depends on reliable knowledge of use conditions and insuring that the test conditions are not set beyond the physical capacity of the materials under test as to promote un-representative failure mechanisms. Values of n may vary from 2-7 with those materials more susceptible to inelastic deformation yielding lower values, Table I[3-16].

Table I. Tabulation of power law exponent from eq. 3 for some common materials.

Failure Mechanism	Power Law Exponent (n)	Author
316 stainless steel	1.5	Halford
solder 97Pb/3Sn	1.9	Norris
solder 37Pb/63Sn	2.27	Kotlowicz
solder 37Pb/63Sn	2.7	Hall
solder 97Pb/3Sn	2.4	Mavoori
Cu and leadframe alloys	2.7	Scharr
Al wire bonds	3.5	Dittmer
ASTM 2024 Al alloy	4.2	Mischke
copper	5	Hatanaka
alumina fracture	5.5	Blish
interlayer dielectic cracking	5.5	Zelenka
Si fracture	5.5	Hagge
Si fracture	7.1	Dunn

The value of temperature amplitude to employ in the model is also dependent on material properties. It is therefore convenient to introduce the concept of a neutral temperature (T_N) to consider when modeling the thermo-mechanical fatigue of materials. The neutral temperature of a material is the temperature at which it exhibits a minimum in stress or changes properties and is important to understand to determine the appropriate form of ΔT to use in the power law model. For a solder this may be its melting point and for a polymer its glass transition temperature. Some failure mechanisms may be accelerated only by a single side of the thermal cycle. These are known as either hot- or cold-side effects. When T_N is above both the use and test temperature of the material the actual temperature amplitude of the test is appropriately employed as the CTE likely changes linearly over this temperature range and does not influence the power-law model. If, however, T_N is below the maximum use and test temperature the stress may change sign (from compression to tension) and or the CTE changes significantly and impacts stress. Such is the case for a polymer that passes through its glass-transition temperature. In these instances the power-law model must be adjusted by biasing for ΔT with respect to T_N. Alternatively, if the fitted data do not behave linearly based on the use and test ΔT, then using a biased ΔT should be considered.

While a good first order approximation, equation (2) does not consider the time-dependent phenomenon present in thermal cycling. Stress relaxation through creep of the die-attach provides for conversion of the elastically stored strain energies to inelastic strain energy, resulting in more fatigue damage per cycle and, therefore, a shorter fatigue life. Returning to Fig. 1., complete stress relaxation during the high temperature dwell would extend the curve at point "A" to the abscissa thereby increasing the area within the hysteresis and energy accumulated for that cycle. Conversely if dwell times are too short, the damage accumulated per cycle decreases, resulting in longer fatigue lives. The effect of dwell time on fatigue life may be considered by incorporating a dwell term into the Coffin-Manson equation:

$$N_f = C(\Delta T)^{-n}\, t_{dwell}^{-m} \tag{4}$$

Considering that dwell time scales with the overall cycle time, and therefore cycle frequency:

$$N_f = C(\Delta T)^{-n}\, f^{m} \tag{5}$$

where the power law exponent for the cycle frequency is typically 1/3[3]. It follows that the acceleration factor becomes:

$$AF = \left(\frac{\Delta T_{use}}{\Delta T_{test}}\right)^{-n}\left(\frac{f_{use}}{f_{test}}\right)^{m} \tag{6}$$

It is of utmost importance to recognize that this acceleration factor pertains to fatigue life, or the number of cycles to failure, and not the time required to complete those cycles. While longer dwell times may lead to shorter fatigue lives, of more practical concern is actual test time; therefore it is useful to consider these relationships with respect to test time:

$$t_{test} = \frac{N_f}{f_{test}} = C(\Delta T)^{-n}\, f_{test}^{m-1} \tag{7}$$

normalizing:

$$\frac{t_2}{t_1} = \left(\frac{\Delta T_2}{\Delta T_1}\right)^{-n}\left(\frac{f_2}{f_1}\right)^{m-1} \tag{8}$$

This expression illustrates that increasing the cycle frequency, or shortening the dwell time effectively decreases test time, even though the number of cycles to complete the test increases, Fig. 3. For instance, while increasing the cycling frequency ten times will more than double the number of cycles to failure, overall test time is decreased over five times.

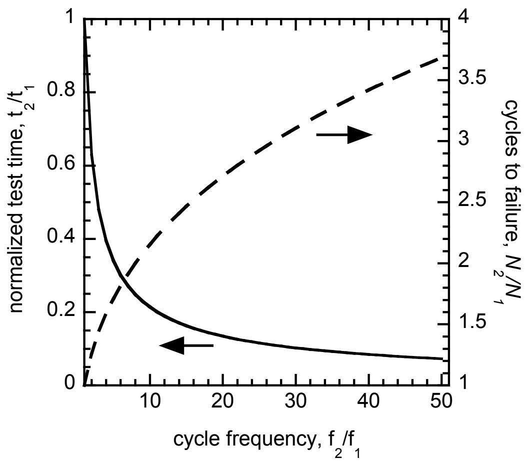

Fig. 3. Illustration of the contrasting trends between fatigue life and test time with increasing cycle frequency.

Modified Coffin-Mason equations have been proposed to empirically address time-dependent parameters observed in different material systems. The Norris-Landzberg equation is presented to compensate for high-temperature damage mechanisms experienced in high lead solders by adding an Arrhenius term:

$$AF = \left(\frac{\Delta T_{use}}{\Delta T_{test}}\right)^{-n} \left(\frac{f_{use}}{f_{test}}\right)^{m} \exp\left[\frac{Q}{R}\left(\frac{1}{T_{use}} - \frac{1}{T_{test}}\right)\right] \quad (9)$$

where Q is the activation energy and R the gas constant. In this form, the activation energy is typically reported as ~ 11.8 kJ/mole and the temperature and frequency power law exponents 1.9 and 1/3, respectively [3]. A lead-free analogue has also been proposed:

$$AF = \left(\frac{\Delta T_{use}}{\Delta T_{test}}\right)^{-n} \left(\frac{t_{use}^{hot}}{t_{test}^{hot}}\right)^{-m} \exp\left[\frac{Q}{R}\left(\frac{1}{T_{use}} - \frac{1}{T_{test}}\right)\right] \quad (10)$$

where the frequency terms are replaced back with a time term t^{hot} which is the ramp plus hot dwell time. In this form, the activation energy is reported as ~13.3 kJ/mole and the temperature and dwell time power law exponents 1.75 and 1/4, respectively[18]. Additional refinements for frequency and temperature dependence have been made to the Coffin-Manson equation [7, 15]. These modifications are also valid starting points for modeling die-attach fatigue life and highlight the necessity for experimental observations.

QUALIFICATION TEST DEVELOPMENT

A test-to-failure protocol is required to deem any reliability information from a thermal cycling sequence. The previously employed term N_f was defined as the number of cycles to failure. This value is more appropriate defined as the mean life to failure and accordingly assigned a probability. For instance N_{50} is the number of cycles through which the probability of failure is 50%. To characterize thermal-cycling failures the two-parameter Weibull distribution is classically employed[19]:

$$F(N) = 1 - \exp\left[-\left(\frac{N}{\theta}\right)^{\beta}\right] \quad (11)$$

Where $F(N)$ is the cumulative failure distribution, N the number of cycles and β and θ the Weibull slope and characteristic Weibull life, respectively. The characteristic Weibull life is the number of cycles by which 63.2% of the population fails. Therefore, when applying the Weibull distribution N_f becomes $N_{63.2}$ and the value employed for the Coffin-Manson style power-law models. The Weibull slope defines the shape of the distribution and has similar values for similar failure mechanisms. Small values of this parameter, $0<\beta<1$, typically denote infant mortalities while larger values, $\beta>3$, denote wear-out mechanisms; accordingly, the Weibull distribution has significant utility in characterizing portions of a bathtub-shape lifetime distribution.

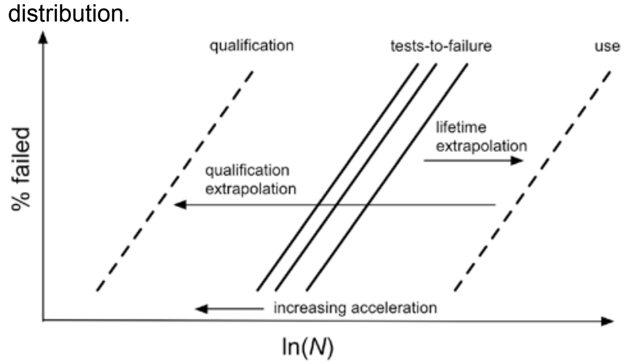

Fig. 4. Schematic probability plot illustrating the philosophical development of a qualification test.

The combination of Coffin-Manson style power-law models and the Weibull distribution can be employed to develop a meaningful thermal-cycling qualification test, Fig. 4. First, several test-to-failure sequences are performed for various cycle parameters, temperature amplitude and cycle frequency, for instance. Next, their failures are fit with the Weibull distribution to determine their characteristic lifetime. With this information the power-law exponents of the Coffin-Manson equation may be calculated and employed to extrapolate these tests to the lower-stress use condition. Ideally, statistics of fielded failures are employed here to further refine the power-law model and deduce the actual lifetime distribution. Alternatively, a safety factor can be used. Finally, the failure distribution is extrapolated to minimize test time (fatigue life) by maximizing the acceleration factor with respect to test time. Further reduction of the qualification-test time is possible by limiting the number of cycles performed for the qualification test. The consequence however is a reduction of the probability that may be assigned to the parts for surviving the desired lifetime.

In the following sections a course of work is set forth en route to developing the first set of test-to-failure protocols described above. This is considered the first step in developing the reliability models for CPV cell assemblies required to design a meaningful and efficient qualification test. System design, control and monitoring are addressed along with a simple infrared imaging method to detect voids within the die-attach layer.

THERMAL CYCLING FOR CPV CELL ASSEMBLIES

The compact nature of concentrator photovoltaics creates unique opportunities, and challenges, for its accelerated testing. Unlike one-sun flat panel PV, CPV typically relies on a die-attach for both electrical and thermal contact. Furthermore, the amount of heat that must dissipate through this joint is much greater and creates one of the largest reliability issues of the module. It is appropriate, therefore, to first consider this feature of the package in a reliability study. The small, repeating components in concentrator PV design lend themselves well to thermal cycling. Reducing the module to these small repeating units provides focus of the evaluation to the components of interest while not compromising their form or function and significantly decreases the thermal mass under test. The result is the possibility for better failure statistics and reduced constraints on the thermal-cycling rate and the required chamber and equipment. The variety in concentrator designs, however, adds a level of complexity to their generic evaluation. For the purpose of this work, a concentrator-cell assembly is defined for the device under test and consists of the CPV cell attached to its substrate with all electrical connections.

The approach employed in the present study is to power cycle the cell assemblies. With the small thermal mass of the cell assemblies, a similarly small forward bias is capable of sufficiently heating the package. In addition to the cell acting as the heating source throughout the test, it also serves as a monitor for package failure. Details on chamber design, control and failure monitoring are presented in the following section.

MATERIALS AND METHODS

Nine CPV-cell assemblies fabricated by Amonix, Inc. were chosen for this investigation. The cell assemblies consisted of a ~1-cm^2 multijunction cell attached to a substrate via several processes. Tabs that extended from the assemblies provided for easy handling and electrical connection. One of the nine assemblies was purposefully modified to simulate a severe failure of the die-attach by removing the majority of this material. Initial characterization of all assemblies consisted of x-ray and infrared imaging.

Infrared imaging of the assemblies was conducted in the following way. An assembly was placed on a water-cooled stage held at 15° C and wired to a DC power supply and current and voltage meters. A burst of 400 infrared images was then taken at the rate of approximately 50 frames/second as a current of 2 A was applied.

The CPV-cell assemblies were then fixtured for thermal cycling. The tabs were used to secure the assemblies into a custom made fixture and make the electrical connections to the cell. This fixture suspends the assemblies to provide for minimum conductive heat flow to the fixture and maximum convective airflow. It also wires the cells in series and provides for voltage monitoring across each cell. Thermocouples were affixed to the bottom of the substrate of each assembly.

The fixtured cell assemblies were placed into the thermal cycling chamber. The chamber consists of a liquid-nitrogen-cooled heat sink and fan. The relatively large thermal mass of the heat sink dictates that it remain at a very low temperature even throughout the high-temperature dwell while no LN2 is flowing, thereby relieving its subsequent cooling demand per cycle. Placement of the fixture approximately 2 cm above the heat sink, and in front of the fan, provides for adequate insulation for heating and convection for cooling.

Heating is enabled by forward biasing the cells. With the cell assemblies wired in series, a DC power supply provides current to the cells according to a proportional-band control between an assigned temperature set point and their average temperature, monitored via the thermocouples placed on the bottom of each substrate. Cooling of the assemblies combines a balance of this current control and actuation of liquid nitrogen through the heat sink and fan, again contingent on the actual and set-point temperatures.

Cycling conditions consisted of a maximum temperature of T_{max}= 110° C, minimum temperature of T_{min}= -40° C and 10-min ramps (15° C/min) between these temperature extremes. These parameters provided for 40-min cycles and a cycle frequency of 36 cycles/ day. Throughout the test, each assembly's temperature, voltage and the applied current were recorded every 20 sec.

RESULTS AND ANALYSIS

Chamber design and control provided for excellent control of assembly temperature. Well-controlled ramp rates of over 30° C/min where achieved for cooling and heating with a current limit of 2.7 A. Presumably, faster heating rates are possible with a higher current limit. Cell-assembly heating for the prescribed thermal-cycling sequence is enabled with the application of a maximum of 2.5 A, and the T_{max} regularly maintained with a current of approximately 2.2 A, Fig. 5.

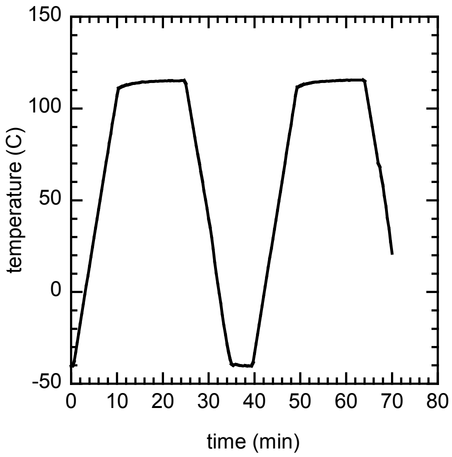

Fig. 5. Measured temperature profile achieved through application of forward bias.

The assembly modified to simulate a failed die-attach was detected within one thermal cycle. During the initial heating ramp, the cell became shunted in a series of steps occurring over two minutes initiating approximately while the assembly was at 20° C and drawing 1-A current, Fig. 6. This cell failure presumably occurred due to the increased thermal resistance between it and the heat-sink, providing for the conditions for thermal runaway.

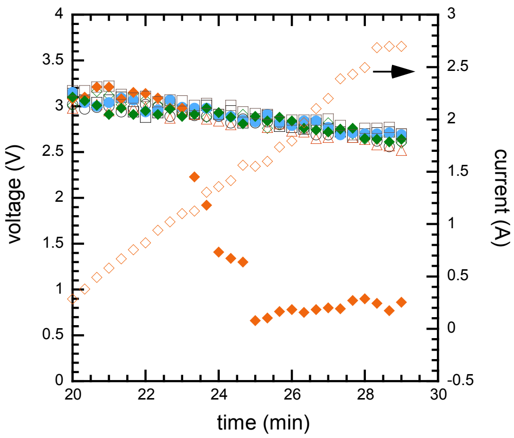

Fig. 6. Voltage, measured across each device, and the series current (orange open diamonds) response of eight cell assemblies highlighting the failure of the modified sample (solid orange diamonds).

It is important to recognize the cell in this case acts as a monitor for the health of the die-attach and subsequent packaging and that its failure is interpreted as a packaging failure rather than a cell failure. A safety written into the controlling software stopped the test when the minimum set temperature of this assembly was not achieved during the first high-temperature dwell, Fig. 7.

The infrared imaging technique is capable of detecting voids in the die-attach. A series of images captured during the forward-bias heating of a cell are presented in Fig. 8. The contrast in these images is such that lighter regions are of higher temperature. By subtracting adjacent images, an image that contains only temperature difference information is obtained circumventing differences in the emissivities of the materials imaged, Fig. 9.

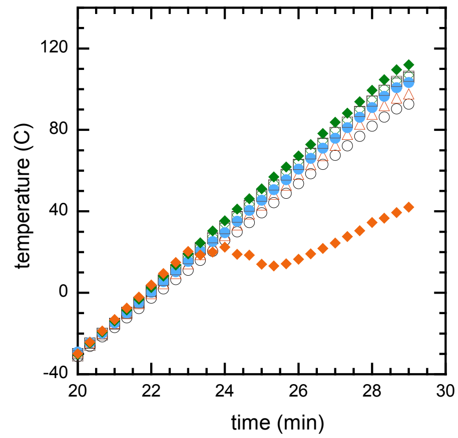

Fig. 7. Temperature response of the eight cell assemblies highlighting the failure of the modified sample (solid orange diamonds).

When a subtracted image is produced at the onset of heating or cooling, a larger temperature difference in the cell above voids in the die-attach is detected. This larger temperature difference manifests from the higher thermal resistance between this section of the cell and heat sink and the time at which the images are taken, before the heat has the opportunity to spread across the cell.

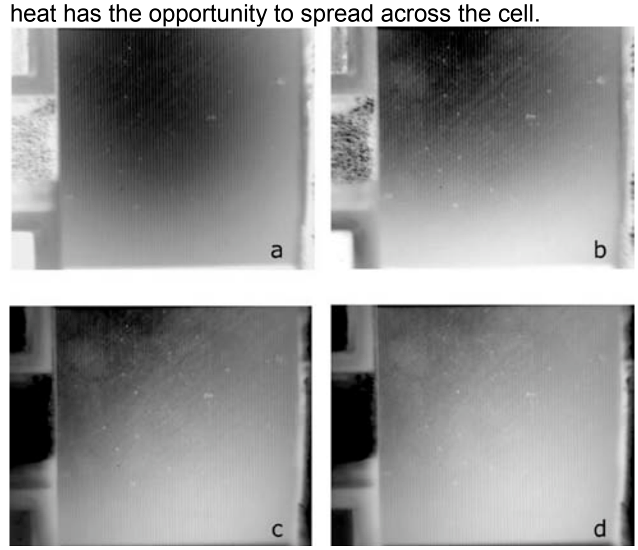

Fig. 8. Infrared images captured during the forward bias heating of a CPV cell. Cell temperature is increasing from frames a-d.

From comparing image pairs similar to that presented in Fig. 9., it appears this infrared technique is capable of detecting voids down to an approximate 200-μm radius. This infrared technique may be subsequently employed periodically through the thermal-cycling sequence to monitor voids in the die-attach.

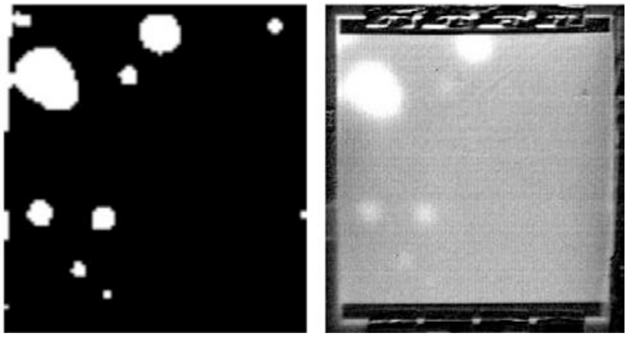
Fig. 9. Pair of x-ray (left) and subtracted infrared images.

CONCLUSION

An approach for developing a meaningful and efficient thermal-cycling qualification test for CPV cell assemblies has been presented. This approach utilizes a test-to-failure protocol, Weibull distribution and Coffin-Manson-style equations to deduce the acceleration factor of the test. Theories on how different parameters and portions of the thermal-cycling sequence affect the acceleration factor were also presented to guide the experimenter in design and modeling of a thermal cycling test. Forward-bias power cycling of CPV-cell assemblies was then demonstrated as an effective method for their thermal cycling. The advantages of this approach were shown to be both the accurate control of temperature, and temperature change, and in-situ failure detection. Finally, an infrared imaging technique capable of detecting a voided die-attach layer was described.

ACKNOWLEDGEMENTS

The authors would like to thank Amonix Inc. for supplying the CPV cell assemblies and x-ray images, and David Albin and Michael Kempe for advice on chamber design and construction. This work was supported by the U.S. Department of Energy under Contract No. DOE-AC36-08GO28308 with the National Renewable Energy Laboratory.

REFERENCES

[1] Ashby MF, Jones DRH. Engineering Materials: An Introduction to Their Properties and Applications. Oxford: Pergamon Press, 1980.
[2] Nelson W. Accelerated Testing: Statistical Models, Test Plans and Data Analyses. New York: John Wiley & Sons, Inc., 1990.
[3] Norris K, Landzberg A. Reliability of Controlled Collapse Interconnections. IBM Journal of Research and Design 1969;13:266.
[4] Kotlowitz RW. Comparative compliance of representative lead designs for surface-mounted components. Components, Hybrids, and Manufacturing Technology, IEEE Transactions on 1989;12:431.
[5] Halford GR, Hirschberg MH, Manson SS. Temperature Effects on the Strainrange Partitioning Approach for Creep Fatigue Analysis. Fatigue at Elevated Temperatures, vol. STP 378. Philadelphia: ASTM, 1972. p.45.
[6] Hall PM. Creep and Stress Relaxation in Solder Joints. In: Lau JH, editor. Aolder Joint Reliability, Theory and Applications. 1991. p.306.
[7] Subrahmanyan R, Wilcox JR, Li CY. A damage integral approach to thermal fatigue of solder joints. Components, Hybrids, and Manufacturing Technology, IEEE Transactions on 1989;12:480.
[8] Dunn CF, McPherson JW. Temperature-cycling acceleration factors for aluminium metallization failure in VLSI applications. Reliability Physics Symposium, 1990. 28th Annual Proceedings., International, 1990. p.252.
[9] Dittmer KJ, Poech MH, Wulff FW, Krumm M. Failure Analysis of Aluminum Wire Bonds in High Power IGBT Modules. Mat. Res. Soc. Proc. 1995;390:251.
[10] Scharr TA. Fatigue properties of base copper materials used in the fabrication of TAB leads. Electronic Components and Technology Conference, 1991. Proceedings., 41st, 1991. p.848.
[11] Mavoori H, Chin J. Reliability, lifetime prediction and accelerated testing of prospective alternatives to lead based solders. Electronic Components and Technology Conference, 1995. Proceedings., 45th, 1995. p.990.
[12] Zelenka RL. A reliability model for interlayer dielectric cracking during temperature cycling. Reliability Physics Symposium, 1991, 29th Annual Proceedings., International, 1991. p.30.
[13] Hatanaka K, Ishimoto Y. An Analysis of Strain Rate Dependent Cyclic Stress-Strain Response and Fatigue Lige in Copper. Adv. Electr. Pkg 1992:813.
[14] Mischke CR. Strength Under Dynamic Conditions. In: Shigley E, Mischke CR, editors. Standard Handbook of Machine Design. McGraw-Hill, 1986. p.13.1*13.9.
[15] Blish RC, III. Temperature cycling and thermal shock failure rate modeling. Reliability Physics Symposium, 1997. 35th Annual Proceedings., IEEE International, 1997. p.110.
[16] Hagge JK. Mechanical considerations for reliable interfaces in next generation electronics packaging. Aerospace and Electronics Conference, 1989. NAECON 1989., Proceedings of the IEEE 1989 National, 1989. p.2021.
[17] Xuejun F, Raiser G, Vasudevan VS. Effects of Dwell Time and Ramp Rate on Lead-Free Solder Joints in FCBGA Packages. Electronic Components and Technology Conference, 2005. Proceedings. 55th, 2005. p.901.
[18] Dauksher W. A Second-Level SAC Solder-Joint Fatigue-Life Prediction Methodology. Device and Materials Reliability, IEEE Transactions on 2008;8:168.
[19] Tobias PA, Trindade DC. Applied Reliability: CRC Press, 1995.

REPORT DOCUMENTATION PAGE	*Form Approved* *OMB No. 0704-0188*

1. REPORT DATE *(DD-MM-YYYY)*	2. REPORT TYPE	3. DATES COVERED *(From - To)*
February 2011	Conference Paper	

4. TITLE AND SUBTITLE	5a. CONTRACT NUMBER
Reliability Testing the Die-Attach of CPV Cell Assemblies	DE-AC36-08GO28308
	5b. GRANT NUMBER
	5c. PROGRAM ELEMENT NUMBER

6. AUTHOR(S)	5d. PROJECT NUMBER
N. Bosco, C. Sweet, and S. Kurtz	NREL/CP-5200-46058
	5e. TASK NUMBER
	PVD9.1330
	5f. WORK UNIT NUMBER

7. PERFORMING ORGANIZATION NAME(S) AND ADDRESS(ES)	8. PERFORMING ORGANIZATION REPORT NUMBER
National Renewable Energy Laboratory 1617 Cole Blvd. Golden, CO 80401-3393	NREL/CP-5200-46058

9. SPONSORING/MONITORING AGENCY NAME(S) AND ADDRESS(ES)	10. SPONSOR/MONITOR'S ACRONYM(S)
	NREL
	11. SPONSORING/MONITORING AGENCY REPORT NUMBER

12. DISTRIBUTION AVAILABILITY STATEMENT

National Technical Information Service
U.S. Department of Commerce
5285 Port Royal Road
Springfield, VA 22161

13. SUPPLEMENTARY NOTES

14. ABSTRACT *(Maximum 200 Words)*

Results and progress are reported for a course of work to establish an efficient reliability test for the die-attach of CPV cell assemblies. Test vehicle design consists of a ~1 cm2 multijunction cell attached to a substrate via several processes. A thermal cycling sequence is developed in a test-to-failure protocol. Methods of detecting a failed or failing joint are prerequisite for this work; therefore both in-situ and non-destructive methods, including infrared imaging techniques, are being explored as a method to quickly detect non-ideal or failing bonds.

15. SUBJECT TERMS

Reliability Testing; CPV; Thermal Cycling; Die-Attach

16. SECURITY CLASSIFICATION OF: a. REPORT	b. ABSTRACT	c. THIS PAGE	17. LIMITATION OF ABSTRACT	18. NUMBER OF PAGES	19a. NAME OF RESPONSIBLE PERSON
Unclassified	Unclassified	Unclassified	UL		19b. TELEPHONE NUMBER *(Include area code)*

Standard Form 298 (Rev. 8/98)
Prescribed by ANSI Std. Z39.18

F1147-E(10/2008)